Tuning the Mechanical Properties of SWNT/Nylon 6,10 Composites with Flexible Spacers at the Interface

ARTICLE *in* NANO LETTERS · MAY 2007

Impact Factor: 13.59 · DOI: 10.1021/nl062868e · Source: PubMed

4 AUTHORS:

Mohammad Moniruzzaman
Saudi Basic Industries Corporation (SABIC)
15 PUBLICATIONS **2,107** CITATIONS
SEE PROFILE

Jayanta Chattopadhyay
Bhabha Atomic Research Centre
92 PUBLICATIONS **1,364** CITATIONS
SEE PROFILE

W. Edward Billups
Rice University
237 PUBLICATIONS **6,191** CITATIONS
SEE PROFILE

Karen I Winey
University of Pennsylvania
331 PUBLICATIONS **11,306** CITATIONS
SEE PROFILE

NANO LETTERS

2007
Vol. 7, No. 5
1178−1185

Tuning the Mechanical Properties of SWNT/Nylon 6,10 Composites with Flexible Spacers at the Interface

Mohammad Moniruzzaman,[†] Jayanta Chattopadhyay,[‡] W. Edward Billups,[‡] and Karen I. Winey*,[†]

Department of Materials Science and Engineering, University of Pennsylvania, Philadelphia, Pennsylvania 19104, and Department of Chemistry, Rice University, Houston, Texas 77005

Received December 7, 2006; Revised Manuscript Received February 19, 2007

ABSTRACT

We have prepared nylon 6,10 nanocomposites using functionalized single wall carbon nanotubes and our interfacial in situ polycondensation method. The specific functional groups $-(CH_2)_nCOCl$ [$n = 4$ and 9] on the sidewalls of SWNT were designed to covalently link nanotubes to the nylon matrix via alkyl segments. The composites with functionalized SWNT show significant improvements in tensile modulus, strength, and toughness relative to nylon and nylon modified with nonfunctionalized SWNT. The alkyl linkages at the SWNT/nylon 6,10 interface contribute significantly to improving the toughness of the composites.

The high aspect ratio, low mass density and outstanding mechanical, electrical, and thermal properties of individual single wall carbon nanotubes (SWNT) and multiwall carbon nanotubes (MWNT) motivate researchers to investigate them as advanced fillers in high strength, lightweight multifunctional polymer nanocomposites. Since the first report of polymer nanocomposite using MWNT by Ajayan et al.,[1] several successful methods have been developed to overcome some fundamental difficulties, e.g., poor dispersion of nanotubes in solvents and polymer matrices, limited load transfer from the matrix to the nanotubes, etc.[2−5] Covalent functionalization of nanotubes is a promising strategy to improve nanotube dispersion in solvents and polymer matrices.[6−8] Covalent functionalization can also provide a means for engineering nanotube/polymer interfaces for optimal composite properties. With respect to mechanical properties, for example, the interfacial adhesion could be modified through covalent or noncovalent interactions between functional groups on nanotubes and the polymer matrix as a way to maximize load transfer. Molecular simulation by Frankland et al.[9] predicted that covalent bonding between SWNT and the polymer matrix with only ∼0.3% grafting density can increase the shear strength of a polymer−nanotube interface by 1 order of magnitude. In this study, we attempt to tune the mechanical properties of SWNT/nylon 6,10 composites by nanoscale design of the SWNT/nylon interface through the introduction of flexible spacers that covalently link the nanotubes and nylon chains. Our approach has simultaneously and significantly improved the tensile modulus, strength, and toughness of the composites.

Nylon 6,10 is a commercially important thermoplastic polyamide. A number of papers have been published recently on nanotube/polyamide composites, mostly using MWNT as the fillers.[10−16] Jia et al.,[10,11] Xia et al.,[12] and Zhang et al.[13,14] fabricated MWNT/nylon 6 composites using different approaches, namely in situ polymerization, microemulsion, and melt-compounding, respectively. Zhang et al. achieved an outstanding 214% improvement in elastic modulus and 162% increase in yield strength by incorporating only 2 wt % MWNT.[14] Compared to MWNT, SWNT have a higher Young's modulus and tensile strength, but fabrication of polymer composites with SWNT is more challenging. The high aspect ratio of SWNT coupled with strong intrinsic van der Waals attractions (∼0.5 eV/nm for SWNT−SWNT contact[8]) produces ropes or bundles that are difficult to disperse in solvents and polymer matrices as compared to MWNT bundles. Moreover, the individual SWNT tubes tend to pull out from ropes or bundles under an applied load, making it difficult to transfer load from the polymer matrix to the nanotubes. Polyamides themselves are also difficult to process. Due to strong intermolecular hydrogen bonds, only a few solvents can dissolve nylons, and the melt processing temperatures are typically very high for commercial nylons (e.g., 270 °C for nylon 6,6). As a result of these difficulties, there are only a few papers that attempt to

* Corresponding author. E-mail: winey@seas.upenn.edu. Telephone: +1 215 8980593. Fax: +1 215 5732128.
[†] University of Pennsylvania.
[‡] Rice University.

10.1021/nl062868e CCC: $37.00
Published on Web 03/31/2007

Scheme 1. Functionalization of SWNT with Alkyl Acid Chloride Group

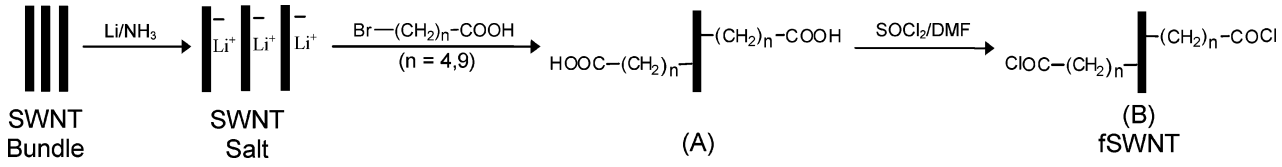

Scheme 2. Synthesis of fSWNT/Nylon 6,10 Composites

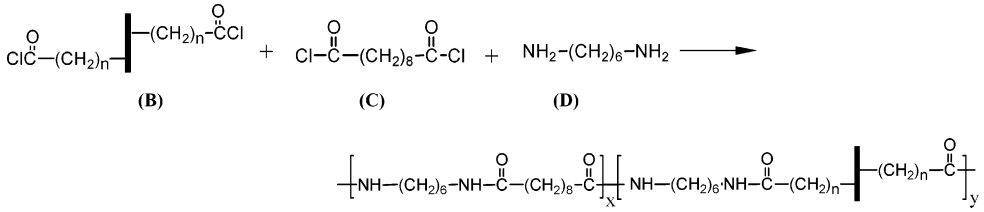

prepare SWNT/nylon composites.[17−19] Gao et al. reported the syntheses of SWNT/ nylon 6 composites using caprolactam both as the monomer and solvent and using carboxylic acid functionalized[17] and amide functionalized[18] SWNT. The resulting composites show good dispersion of SWNT and significant improvements in Young's modulus and tensile strength (e.g., 153% increase in Young's modulus and 103% increase in tensile strength with 1 wt % carboxylated SWNT) due to the grafting of nylon chains on SWNT.

In this study, our interfacial in situ polycondnesation method[19,20] was adapted to synthesize nylon 6,10 composites with functionalized SWNT, as well as pristine SWNT. This polycondensation method involves an aqueous and an organic phase, each carrying one of the two highly reactive monomers (a diacid halide and a diamine). The two phases for the interfacial polycondensation are brought together with or without stirring. Haggenmueller et al.[19,20] prepared SWNT/ nylon 6,6 composites using a stirred system, whereas Kang et al.[16] prepared MWNT/nylon 6,10 composites using an unstirred system (the familiar nylon rope trick). We have carried out the interfacial polycondensation with stirring, because it offers several advantages over the unstirred system: wider choice of organic solvents as it does not require the formation of a tough film at the interface, comparatively higher molecular weight polymers (due to more interfacial area), and improved dispersion of nanotubes. In the fabrication of nanotube/nylon composites, an important drawback of the unstirred system is the loss of a significant quantity of monomers and nanotubes while grasping and drawing the film from the interface, therefore making it difficult to quantify the wt % of nanotubes in the composites. We fabricate the composite with nylon 6,10, because the diacid chloride used in this synthesis (sebacoyl chloride) is less reactive to water (a necessary phase in this method) and unlike nylon 6,6, there is no report of cyclic oligomer formation during this polycondensation reaction.

There are only a few reports in the literature that functionalize SWNT sidewalls with alkyl groups[21,22]or alkyl carboxylic acid groups.[23] Peng et al.[23] added short alkyl chains ($n = 2$ and 3) with terminal carboxylic acid groups to the SWNT sidewall by the reaction of SWNT with diacyl peroxides. Here, we achieve sidewall functionalization of SWNT with long chain carboxylic acid groups using a modified Birch-type reaction protocol, which was originally developed by Liang et al.[21] to functionalize SWNT with long alkyl chains. The nanotubes were first functionalized with long chain carboxylic acid groups, $-(CH_2)_n-COOH$ ($n =$ 4 and 9) by reacting with bromo-carboxylic acid in liquid ammonia in the presence of lithium metal, Scheme 1. The carboxylic acid groups were then converted into acid chloride groups by reacting with thionyl chloride. For convenience, the acid chloride functionalized nanotubes, fSWNT (B in Scheme 1) with $n = 4$ and 9 are designated as C4-SWNT and C9-SWNT, respectively, whereas the unfunctionalized nanotubes are designated as SWNT.

It is well-known that the polycondensation reaction between hexamethylenediamine and sebacoyl chloride yields nylon 6,10. We have carried out this polycondensation reaction in the presence of fSWNT (C4-SWNT and C9-SWNT) to synthesize fSWNT/nylon 6,10 composites, Scheme 2. We expect that in the composites with C4-SWNT and C9-SWNT, nanotubes will be covalently integrated into nylon chains.

There are several variables in this reaction: (i) the length of the alkyl chains on the functionalized nanotubes (n), (ii) the ratio of the diacid chloride to the nanotubes, and (iii) the grafting density of the functional groups on the tubes. In this study, we have examined the effect of the first two variables. For a comparative study, the unfunctionalized SWNT were also used in the nylon synthesis and composite fabrication.

Functionalization of SWNT. SWNT were synthesized by a high-pressure carbon monoxide method (HiPco) at Rice University.[24] SWNT were purified[25] and have residual metal less than 6 wt % as measured by thermogravimetric analysis (TGA). In order to functionalize the sidewall of SWNT with long chain carboxylic acid groups, 100 mg of SWNT (8.3 mmol of carbon) were taken into a dry 1000 mL three neck round-bottom flask fitted with a dry ice condenser under an atmosphere of argon. Ammonia (600 mL) was then condensed into the flask followed by the addition of lithium metal (Aldrich, 600 mg, 8.5 mmol). The suitable bromocarboxylic acid (5-bromovaleric acid; 1.3 equiv. and 10-bromodecanoic acid; 3 equiv., Aldrich) was then added and

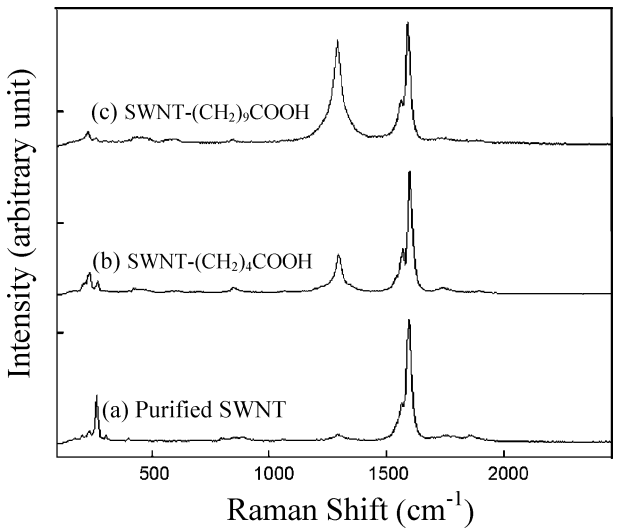

Figure 1. Raman spectra of purified and long chain carboxylated SWNT.

the mixture was stirred at −33 °C for 12 h with slow evaporation of ammonia. The flask was then cooled in an ice bath, and the reaction mixture was quenched by the slow addition of ethanol (15 mL) followed by water (20 mL). The reaction mixture was acidified with 10% HCl, and the nanotubes were extracted into hexane and washed several times with water. The hexane layer was then filtered through a 0.2 μm PTFE membrane and washed successively with ethanol and chloroform. The functionalized SWNT were dried overnight in vacuo at 80 °C.

To convert the carboxylic acid groups into acid chloride groups, 200 mg of carboxylated SWNT and 30 mL freshly distilled benzene were taken into a 100 mL round-bottom flask fitted with a reflux condenser and a magnetic stir bar. To this mixture were added successively 20 mL of $SOCl_2$ (99.5%, Acros) and 2 mL of DMF. The suspension was stirred at 65 °C for 24 h. The solid was then separated by filtration in a 0.2 μm PTFE membrane filter paper and washed thoroughly with anhydrouos tetrahydrofuran (THF). Finally, the solid was vacuum-dried at room temperature for 4 h.

Functionalized SWNT were characterized with a Renishaw micro-Raman spectrometer, a Perkin-Elmer 2000 FTIR spectrometer, an X-ray photoelectron spectrometer (XPS), and an SDT 2960 DTA/TGA analyzer (TA instruments). Raman spectra from solid samples of SWNT and the carboxylated SWNT were collected with excitation at 780 nm. The Raman spectrum of pristine SWNT exhibit a tangential mode at 1590 cm^{-1} (G band) and radial breathing modes at 213, 230, and 265 cm^{-1}, which indicates a diameter distribution of HiPco SWNT, Figure 1a. After functionalization, the relative intensity of the disorder mode (D band) at 1290 cm^{-1} is enhanced as groups are attached to the sidewall of the nanotubes, Figure 1, panels b and c. This is due to the chemically induced disruption of sp^2-hybridized carbons in the hexagonal framework of the nanotubes wall. Raman spectroscopy clearly indicates the successful covalent functionalization of the SWNT.

FTIR spectra of the alkyl carboxylic acid functionalized tubes show the C═O stretching vibration at 1710 cm^{-1}, which shifted to 1790 cm^{-1} when the carboxylic acid groups were converted to the acid chloride group. The XPS analysis of C4-SWNT and C9-SWNT indicates the chlorine content to be 2−3%, as expected.

Thermogravimetric analysis (TGA) of the functionalized SWNT was used to measure the extent of functionalization, which directly gives information about the carbon/functional group ratio. Samples were degassed at 80 °C and then heated 10 °C/min to 800 °C and held there for 30 min. On the basis of the weight loss at 150−500 °C during TGA experiments, there is one alkyl acid chloride group for every 35 and 32 carbon atoms of the nanotube for C4-SWNT and C9-SWNT, respectively.

The length and diameters of the nanotubes were determined from tapping mode atomic force microscopy (AFM) images of the tubes as deposited on silicon wafers from suspensions.[26,27] The average length of the purified HiPco SWNT was 230 ± 95 nm, as determined from the AFM images. After functionalization with long chain carboxylic acid groups, the average length did not change significantly, which indicates that the functionalization protocol used in this study does not adversely affect the nanotube length. The average diameter of the carboxylated SWNT bundle was ∼6−7 nm, indicating that the SWNT are present in the form of small bundles after functionalization. The slight bundling of SWNT after the functionalization could be attributed to the intermolecular hydrogen bonding of carboxylic acids.

Synthesis of Nylon 6,10 and SWNT/Nylon 6,10 Composites. The organic phase of our interfacial polycondensation reaction contained the diacid chloride (sebacoyl chloride (99.5%, Acros)) and the suspended nanotubes. The aqueous phase contained the diamine (1,6-hexamethylene diamine (Fluka)) and a base sodium hydroxide to neutralize the byproduct of this reaction, hydrochloric acid. Ideally, the organic phase for this polycondensation method should be immiscible with water and be able to disperse the SWNT and fSWNT. These two criteria were best fulfilled by the solvent dichlorobenzene. The aqueous to organic phase volume ratio and the diamine concentration was optimized to maximize yield.

For the polymerization of neat nylon 6,10, 1.4 g (0.011 mol) of hexamethylene diamine and 0.88 g (0.022 mol) of sodium hydroxide was dissolved in 110 mL water and was placed in a blender (Waring, model 51BL31). A total of 2.63 g (2.36 mL, 0.011 mol) of sebacoyl chloride was dissolved in 190 mL of dichlorobenzene. The blender was turned on at the highest speed, and the sebacoyl chloride solution was quickly added to the diamine solution. The reaction was very fast and typically ran for just 3 min. The reaction was terminated by adding a 3% aqueous hydrochloric acid solution to the blender, and the stirring was continued for 1 min more. The polymer was filtered through a 10 μm PTFE membrane (Millipore Mitex), washed repeatedly with water and acetone, and dried at 100 °C under vacuum for 24 h.

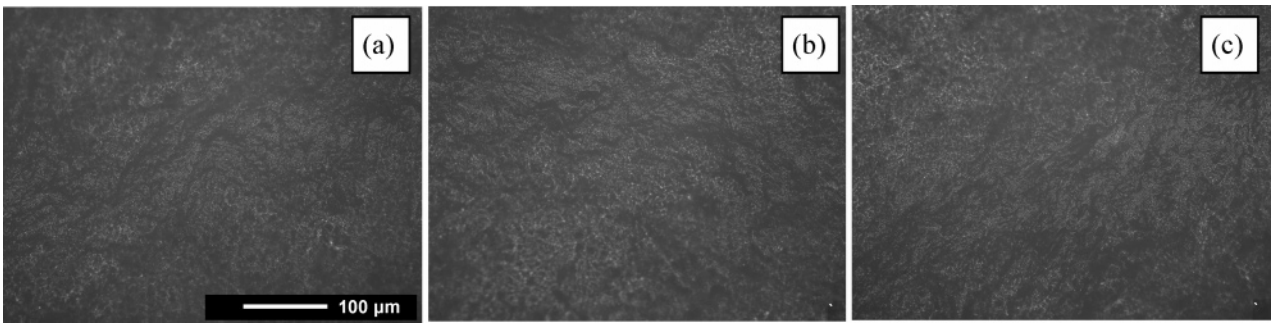

Figure 2. Optical micrographs of 0.5 wt % nanotube/nylon 6,10 composites. (a) SWNT/nylon, (b) C4-SWNT/nylon, and (c) C9-SWNT/nylon.

Scheme 3. Reaction between Hexamethylene Diamine and C9-SWNT

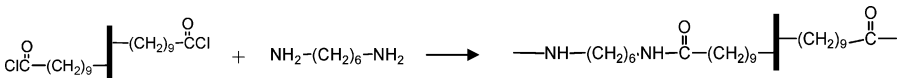

To synthesize the nanotube/nylon 6,10 composites, different wt % nanotubes were first dispersed in dichlorobenzene with the aid of bath ultrasonication for 24 h, and then sebacoyl chloride was added to the suspension. The reaction was then carried out using the same procedure and reagent ratios, as described for the nylon 6,10 synthesis. Composites with 0.05, 0.1, 0.5, and 1 wt % loadings of nanotubes were prepared. For C4-SWNT and C9-SWNT, the loading of the nanotubes represent the wt % of the tubes with the functional groups.

The reaction product of the interfacial polymerization of nylon 6,10 was a white powder. The maximum yield (~80%) was obtained with a 1:2 volume ratio of aqueous to organic phase and with a diamine concentration that was 10% excess of the stoichiometric ratio. FTIR confirmed the chemical structure of the nylon 6,10, showing absorptions for all of the required chemical groups:[28] N−H stretch at 3309 cm^{-1}, C−H stretch at 2853−2930 cm^{-1}, amide-I at 1638 cm^{-1}, and amide-II at 1542 cm^{-1}. The nanotube/nylon composites were black powders, with no visible phase separation of nylon 6,10 and nanotubes. The Mark−Houwink equation, $[\eta] = K_v(\bar{M}_v)^a$ was used to determine the viscosity averaged molecular weight, $\bar{M}_v$, from intrinsic viscosity measurements (using $K_v = 1.35 \times 10^{-4}$ and $a = 0.96$, for nylon 6,10 in *m*-cresol at 25 °C),[29] resulting in a $\bar{M}_v \sim 18\,000$ g/mol. The presence of SWNT did not affect the molecular weight of the resulting nylon. The presence of fSWNT slightly reduced the molecular weight of the resulting nylon ($\bar{M}_v \sim 16\,000$ g/mol in 1 wt % composites).

Dispersion of Nanotubes in the Composites. Good dispersion of nanotubes in a polymer matrix provides more uniform stress distribution,[3] minimizes the presence of stress-concentration centers, and increases the interfacial area for stress transfer from the polymer matrix to the nanotubes. Haggenmueller et al. showed that interfacial in situ polymerization in a stirred system produces nanocomposites with good nanotube dispersion, provided the nanotubes are well-dispersed in the suspension prior to polymerization.[19] Pristine SWNT are well dispersed in dichlorobenzene (DCB) with the aid of ultrasonication,[30] as are C4-SWNT and C9-SWNT in this study.

To evaluate the dispersion of nanotubes in the composites, films of nanotube/nylon composites (with thickness of about 0.4 mm) were prepared by compression molding in a press at 230 °C, followed by quenching on an aluminum bar. The optical micrographs (Olympus, BH-2, reflection mode) of nylon 6,10 composites with 0.5 wt % SWNT, C4-SWNT, or C9-SWNT show good dispersion of nanotubes on the length scale of optical microscopy, Figure 2. Therefore, interfacial in situ polycondensation in a stirred system is capable of preserving the good nanotube dispersion of suspensions into the polymer nanocomposites.

Evidence of Covalent Bonding in the Composites. One of the main objectives of this study was to take advantage of the covalent bonding between the nanotubes and the nylon chains. To investigate whether the acid chloride functionalized nanotubes form covalent bonds with the nylon chains, C9-SWNT were dispersed in dichlorobenzene without the diacid monomer and reacted with an excess of aqueous diamine solution (Scheme 3). After the reaction, the excess diamine was washed away, and the reaction product was investigated by FT-IR. The FTIR spectrum shows the amide C═O and NH stretching bands at 1638 and 3390 cm^{-1}, respectively (Figure 3). The appearance of these two peaks

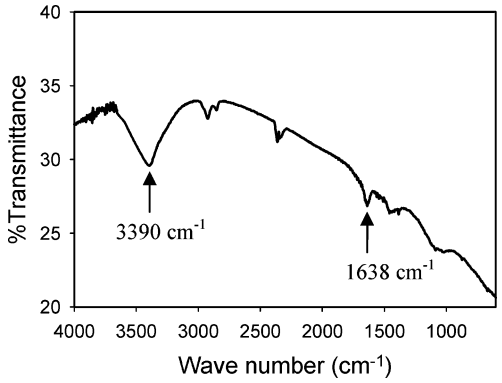

Figure 3. FTIR of the reaction product from Scheme 3.

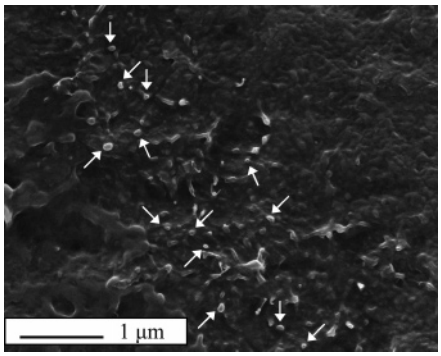

Figure 4. SEM image of the fracture surface of 0.5 wt % C4-SWNT/nylon 6,10 composite film. The arrows in the figure indicate the protruding, broken nanotube bundles. The features in SEM appear larger than the SWNT bundles; see text.

along with the disappearance of the acid chloride carbonyl stretching peak (1790 cm^{-1}) confirms the covalent bond formation between the functionalized SWNT and nylon 6,10 in the composite.

Further evidence of covalent bonding between nanotubes and nylon chains comes from the solubility of the composites and fracture surface analysis of the composite films. The nanotubes functionalized with the alkyl acid chloride groups showed very poor dispersion in formic acid, which is a good solvent for nylon 6,10. In contrast, a stable suspension forms when the composite is dissolved in formic acid. The change in solubility or dispersability of nanotubes after the composite synthesis is indirect proof that there are covalent bonds between the nanotubes and the nylon molecules.

Composite films were fractured in liquid nitrogen, sputtered with a thin layer of Au/Pd (60:40), and imaged at 15 kV in a scanning electron microscopy (SEM) (JEOL 6300FV). Figure 4 shows the SEM image of the fracture surface of the composite film containing 0.5 wt % C4-SWNT. In the SEM image, the SWNT bundles appear as bright regions due to their high electrical conductivity. From TEM analysis of a similar bright SEM feature on a fracture surface of SWNT/nylon 6 composites, Gao et al.[17] showed that the bright spots do not represent the actual bundle size of SWNT, but rather they include the SWNT and the polymer that is closely associated with SWNT. The fracture surfaces of our composite films predominately show broken nanotube bundles, indicating strong interfacial bonding between the nylon and nanotubes in the polymer composites.

Mechanical Properties of Nanotube/Nylon 6,10 Composite Fibers. Fibers of the composites (80−100 μm diameter) were fabricated by melt extrusion at 240 °C using a DACA SpinLine with a spinneret diameter of 500 μm. The mechanical properties of the composite fibers were evaluated using an Instron 5564 instrument, with a gauge length of 25.4 mm and crosshead speed of 2 mm/min.

Figure 5 shows the stress−strain curves of nylon 6,10 and the composite fibers containing 1 wt % SWNT, C4-SWNT, or C9-SWNT. The Young's modulus, ultimate tensile strength, toughness, and strain at break of nylon 6,10 and the composite fibers with 1 wt % nanotubes are listed in

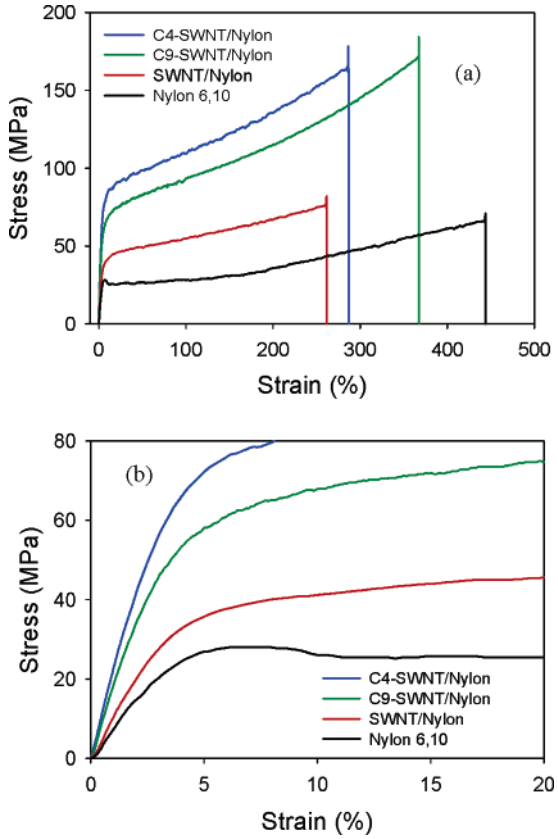

Figure 5. (a) Stress−strain curves of composite fibers containing 1 wt % SWNT and fSWNT. (b) As above, replotted to show the differences in Young's modulus.

Table 1. Mechanical Properties of Nylon 6,10 Fibers and 1 wt % Nanotube/nylon 6,10 Composite Fibers

	nylon 6,10	SWNT	C4-SWNT	C9-SWNT
Young's modulus (MPa)	879 ± 65	1217 ± 86	2309 ± 78	1955 ± 73
% change		38	162	132
tensile strength (MPa)	67 ± 6	79 ± 7	168 ± 7	177 ± 6
% change		17	149	163
toughness (MPa)	177 ± 18	152 ± 21	365 ± 21	417 ± 24
% change		−14	106	136
strain at break (%)	440 ± 7	262 ± 5	290 ± 6	368 ± 7

Table 1. The nylon 6,10 fibers synthesized and fabricated in our lab have a Young's modulus of 879 MPa and a tensile strength of 67 MPa. All of the SWNT and fSWNT composite fibers with 1 wt % fill have higher Young's modulus and higher tensile strength than pure nylon 6,10 and the improvement is more pronounced with fSWNT. Composite fibers with C4-SWNT exhibit the highest Young's modulus, 2309 MPa, which is 162% higher than that of the nylon 6,10 fibers. This outstanding improvement occurs at just 1 wt % C4-SWNT loading in the composite and is coupled with substantial increases in tensile strength (149%) and toughness (106%). The improvements found by incorporating 1 wt % C9-SWNT are even greater for toughness (136%) and strain at break.

Improvements in tensile strength and modulus in most of the reported nanotube/polymer composites are coupled with a reduction in strain at break, indicating a decrease in

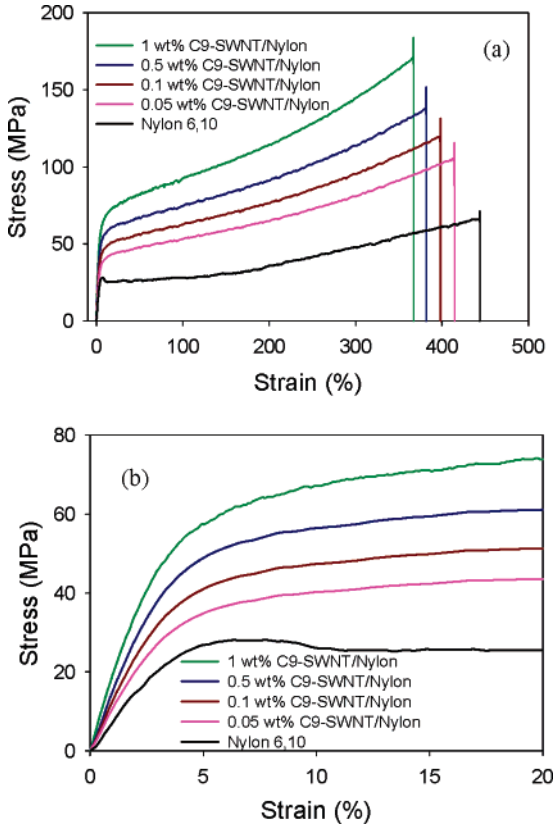

Figure 6. (a) Stress−strain curves of nylon 6,10 and C9-SWNT/nylon composite fibers with 0−1 wt % C9-SWNT. (b) As above, replotted to show differences in Young's modulus.

polymer toughness and flexibility.[2,4] For example, Gao et al. found that in their melt spun SWNT/nylon 6 composite fibers, the Young's modulus increases from 440 to 575 MPa (31%), the tensile strength increases from 40.9 to 69.1 MPa (69%), whereas the break at strain decreases from 417% to 250% with the incorporation of 1 wt % pristine SWNT in nylon 6.[18] In our study, incorporation of 1 wt % pristine SWNT in nylon 6,10 reduces the break at strain from 440% to 262%, but when C9-SWNT are incorporated into nylon 6,10, the strain at break improves significantly to 368%. The toughness of the composite fibers increases progressively from the composite with pristine SWNT to the fSWNT with increasing alkyl chain length in the functional moiety. Thus, covalent bonding between the nanotube and the nylon chains with flexible spacers at the nanotube/nylon interface improves the Young's modulus, tensile strength, and toughness with minimal reduction in the strain at break. The composite fibers with longer alkyl segment ($n = 9$) at the nanotube/nylon interface show the highest strain at break and toughness, whereas the fibers with shorter alkyl segment ($n = 4$) at the nanotube/nylon interface exhibit the highest Young's modulus.

Figure 6 shows the stress−strain curves of C9-SWNT/nylon composite fibers with nanotube loadings, from 0.05 to 1.0 wt %. The Young's modulus, tensile strength, and toughness improve steadily as the C9-SWNT loading increases from 0.05 to 1 wt %, Table 2, suggesting that higher loadings might provide still more property enhancement. Coupled with these improvements in Young's modulus, tensile strength, and toughness, there are only modest reductions in the strain-at-break of the composites. As expected, the strain-at-break decreases gradually with increasing nanotube loadings, but these reductions are significantly less pronounced than commonly reported for SWNT/polymer composites.[2,4] Therefore, our fabrication strategy, which successfully manipulates the SWNT/nylon interface, is a promising way of achieving greatly improved mechanical properties, without compromising toughness and flexibility.

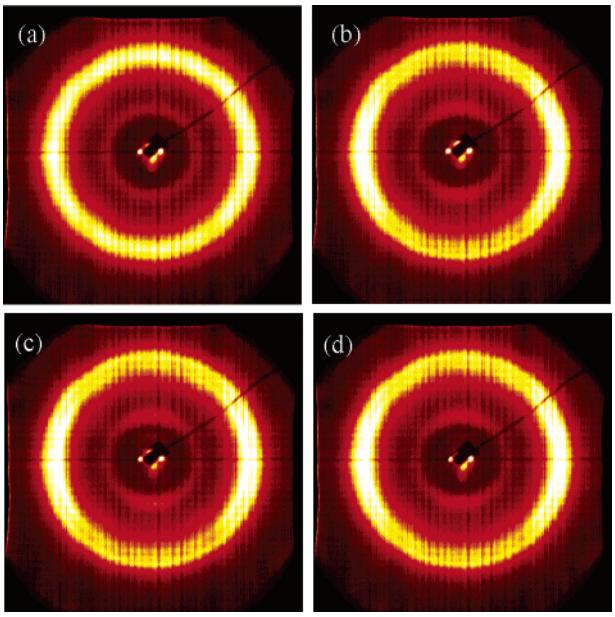

Figure 7. 2D wide-angle X-ray scattering patterns from (a) nylon 6,10 fibers, (b) 1 wt % SWNT/nylon fibers, (c) 1 wt % C4-SWNT/nylon fibers, and (d) 1 wt % C9-SWNT/nylon fibers. Fiber direction is along the meridian.

The question arises as to the origin of the increased toughness of the C9-SWNT/nylon composite fibers relative to SWNT and C4-SWNT composite fibers. Several factors can contribute to the mechanical properties of nanotube/nylon composites: matrix morphology, filler orientation, filler distribution, and load transfer at the matrix−filler interface. As mentioned earlier, all of the composites in this study show similar dispersion of nanotubes, irrespective of the type of the nanotubes. To evaluate the nylon morphology and the nanotube orientation, X-ray scattering was performed in transmission using our multiple-angle X-ray scattering (MAXS) apparatus equipped with a 2-D wire detector.[31,32]

The 2D wide-angle X-ray diffraction patterns show that both the nylon fibers and the nanotube/nylon fibers exhibit a lower angle reflection at $2\theta = \sim 10°$, which corresponds to the amide−amide distance, and two higher angle reflections at $2\theta = 20-24°$, Figure 7. Thus, the presence of nanotubes in these nylon 6,10 melt extruded fibers does not significantly alter the nylon crystal structure of the nylon. However, the introduction of nanotubes does significantly increase the anisotropy of the nylon matrix as evidenced by the low and high angle peaks becoming more intense at the meridional and equatorial positions, respectively. Our recent study of SWNT/polyethylene composites indicates that SWNT nucleate and template polymer crystallization.[32] Thus,

Table 2. Mechanical Properties of C9-SWNT/nylon 6,10 Composite Fibers

	0 wt % of C9-SWNT	0.05 wt % of C9-SWNT	0.1 wt % of C9-SWNT	0.5 wt % of C9-SWNT	1 wt % of C9-SWNT
Young's modulus (MPa)	879 ± 65	1148 ± 52	1350 ± 60	1620 ± 67	1955 ± 73
% change		31	54	84	125
tensile strength (MPa)	67 ± 6	105 ± 5	124 ± 6	145 ± 7	177 ± 6
% change		56	84	115	163
toughness (MPa)	177 ± 18	284 ± 16	311 ± 19	350 ± 21	417 ± 24
% change		60	76	98	136
strain at break (%)	440 ± 7	413 ± 7	399 ± 6	383 ± 6	368 ± 7

after the extensional flow aligns the SWNT in the flow direction, the nylon crystallizes anisotropically with the nylon chains preferentially along the fiber direction. Azimuthal scans of the low angle peak were fit with Gaussian functions, and the full widths at half-maximum (fwhm) are used to quantify the extent of nylon orientation. The 1 wt % nanotube/nylon 6,10 composite fibers containing SWNT, C4-SWNT, and C9-SWNT have fwhms of 63°, 65°, and 61°, respectively. Thus, we conclude that the nylon matrix morphology, both with respect to crystalline structure and orientation, is indistinguishable in these nanotube/nylon composite fibers.

Regarding nanotube orientation, we use small-angle X-ray scattering to detect the form factor scattering of the nanotube bundles at a q range of 0.015−0.075 $Å^{-1}$.[31,32] Here the azimuthal scans were fit with Lorenztians and the 1 wt % nanotube/nylon 6,10 composite fibers containing SWNT, C4-SWNT, and C9-SWNT have fwhms of 65°, 62°, and 67°, respectively, indicating that the composite fibers have comparable nanotube orientation. As the SWNT, C4-SWNT, and C9-SWNT composite fibers possess indistinguishable matrix morphology, filler orientation, and filler distribution, we conclude that the improved toughness of the C9-SWNT/nylon composite fibers originates from differences at the nanotube/nylon interface.

The amide groups, −NH−CO−, in nylon chains exist almost exclusively in the trans-conformation, and their H-bonding renders them substantially stiffer than $-CH_2-CH_2-$ groups.[33] In nanotube/nylon nanocomposites, direct covalent bonds between the nanotubes and nylon chains via amide linkages[15,18] reduce the flexibility of the nylon matrix. In contrast, covalent bonding between nanotubes and nylon chains via alkyl segments in our C4-SWNT and C9-SWNT composites provides improved chain flexibility at the critical SWNT/matrix interface. These alkyl segments adopt different conformations under an applied stress, and longer alkyl chains can adopt more conformations. Thus, the variety of chain conformations of the interfacial alkyl segment in C9-SWNT/nylon composite fibers permits larger deformations, so that more energy is dissipated before fracture. Although the shorter alkyl segments at the C4-SWNT/nylon interface can adopt comparatively fewer conformations, the stress transfer from the nylon to the nanotubes appears to be more efficiently, which results in a higher modulus.

In summary, we have synthesized nylon 6,10 nanocomposites with functionalized SWNT using our interfacial in situ polycondensation method. HiPco SWNT were functionalized with alkyl acid chloride groups for the nanoscale manipulation of the nanotube/nylon interface. We have optimized the reaction parameters to get a good yield (∼80%) of the composites. The composites exhibit good dispersion of the nanotubes on the length scale of optical microscopy. The presence of covalent bonds between the nanotubes and the nylon chains has been shown by FT-IR. As a result of this covalent bonding, the fSWNT/nylon 6,10 composite fibers exhibit high Young's modulus, high tensile strength, and high toughness. The functionalized SWNT with long alkyl chains ($n = 9$) on the surface produce tougher composite fibers, whereas SWNT with shorter alkyl chains ($n = 4$) produce higher modulus composite fibers. The improved toughness of the composite fibers arises from the ability of adopting different conformations under stress by the flexible spacers at the nanotube/nylon 6,10 interface. These results demonstrate methods for tailoring the mechanical properties in nanotube/polymer composites by designing appropriate covalent linkages between the nanotubes and the matrix polymer.

Acknowledgment. The authors acknowledge financial support from the National Science Foundation (DMR-MRSEC 05-20020, CHE-0450085), the Office of Naval Research (DURINT N00014-00-1-0720), and the Robert A. Welch Foundation (C-0490). M.M. is supported by a postdoctoral fellowship from the Natural Science and Engineering Research Council of Canada. We thank Lai-Ching Chou for assisting with the X-ray scattering experiments.

Supporting Information Available: FT-IR spectra of the long chain carboxylated SWNT and nylon 6,10; the tapping mode AFM image of the carboxylated SWNT; X-ray intensity vs 2θ plot from the 2D diffraction patterns of nylon and composite fibers. This material is available free of charge via the Internet at http://pubs.acs.org

References

(1) Ajayan, P. M.; Stephan, O.; Colliex, C.; Trauth, D. *Science* **1994**, *265* (5176), 1212−14.
(2) Moniruzzaman, M.; Winey, K. I. *Macromolecules* **2006**, *39*, 5195−5205.
(3) Coleman, J. N.; Khan, U.; Gun'ko, Y. K. *Adv. Mater.* **2006**, *18*, 689−706.
(4) Miyagawa, H.; Misra, M.; Mohanty, A. K. *J. Nanosci. Nanotechnol.* **2005**, *5* (10), 1593−1615.

(5) Du, F.; Winey, K. I. In *Nanomaterials Handbook*; Gogotsi, Y., Ed.; CRC Press: Boca Raton, FL, 2006; pp 565−582.
(6) Sun, Y.-P.; Fu, K.; Lin, Y.; Huang, W. *Acc. Chem. Res.* **2002**, *35* (12), 1096−104.
(7) Dyke, C. A.; Tour, J. M. *Chem. Eur. J.* **2004**, *10* (4), 812−817.
(8) Dyke, C. A.; Tour, J. M. *J. Phys. Chem. A* **2004**, *108* (51), 11151−11159.
(9) Frankland, S. J. V.; Caglar, A.; Brenner, D. W.; Griebel, M. *J. Phys. Chem. B* **2002**, *106* (12), 3046−3048.
(10) Jia, Z.; Xu, C.; Liang, J.; Wei, B.; Wu, D.; Zhu, C. *Xinxing Tan Cailiao* **1999**, *14*, 32−36.
(11) Jia, Z.; Wang, Z.; Xu, C.; Liang, J.; Wei, B.; Wu, D.; Zhang, Z. *Qinghua Daxue Xuebao, Ziran Kexueban* **2000**, *40*, 14−16.
(12) Xia, H.; Wang, Q.; Qiu, G. *Chem. Mater.* **2003**, *15*, 3879−3886.
(13) Zhang, W. D.; Shen, L.; Phang, I. Y.; Liu, T. X. *Macromolecules* **2004**, *37*, 256−259.
(14) Liu, T.; Phang, I. Y.; Shen, L.; Chow, S. Y.; Zhang, W. D. *Macromolecules* **2004**, *37*, 7214−722.
(15) Zheng, H.; Gao, C.; Wang, Y.; Watts, P. C. P.; Kong, H.; Cui, X.; Yan, D. *Polymer* **2006**, *47*, 113−122.
(16) Kang, M.; Myung, S. J.; Jin, H. J. *Polymer* **2006**, *47*, 3961−3966.
(17) Gao, J.; Itkis, M. E.; Yu, A.; Bekyarova, E.; Zhao, B.; Haddon, R. C. *J. Am. Chem. Soc.* **2005**, *127* (11), 3847−3854.
(18) Gao, J.; Zhao, B.; Itkis, M. E.; Yu, A.; Bekyarova, E.; Hu, H.; Kranak, V.; Yu, A.; Haddon, R. C. *J. Am. Chem. Soc.* **2006**, *128* (11), 7492−7496.
(19) Haggenmueller, R.; Du, F.; Fischer, J. E.; Winey, K. I. *Polymer* **2006**, *47*, 2381−2388.
(20) Winey, K. I.; Haggenmueller, R.; Du, F. U.S. Patent 2003, US 2003180526-A1; US7148269-B2.
(21) Liang, F.; Sadana, A. K.; Peera, A.; Chattopadhyay, J.; Gu, Z.; Hauge, R. H.; Billups, W. E. *Nano Lett.* **2004**, *4* (7), 1257−1260.
(22) Ying, Y.; Saini, R. K.; Liang, F.; Sadana, A. K.; Billups, W. E. *Org. Lett.* **2003**, *5*, 1471.
(23) Peng, H.; Alemany, L. B.; Margrave, J. L.; Khabashesku, V. N. *J. Am. Chem. Soc.* **2003**, *125*, 15174−15182.
(24) Bronikowski, M. J.; Willis, P. A.; Colbert, D. T.; Smith, K. A.; Smalley, R. E. *J. Vac. Sci. Technol. A* **2001**, *19*, 1800.
(25) Chiang, I. W.; Brinson, B. E.; Huang, A. Y.; Willis, P. A.; Bronikowski, M. J.; Margrave, J. L.; Smalley, R. E.; Hauge, R. H. *J. Phys. Chem. B* **2001**, *105*, 8297−8301.
(26) Star, A.; Stoddart, J. F.; Steuerman, D.; Diehl, M.; Boukai, A.; Wong, E. W.; Yang, X.; Chung, S.-W.; Choi, H.; Heath, J. R. *Angew. Chem., Int. Ed.* **2001**, *40*, 1721−1725.
(27) Islam, M. F.; Rojas, E.; Bergey, D. M.; Johnson, A. T.; Yodh, A. G. *Nano Lett.* **2003**, *3*, 269−273.
(28) Kohan, M. I., Ed.; *Nylon Plastics*; Wiley: New York, 1973.
(29) Morgan, P. W.; Kwolek, S. L. *J. Polym. Sci. A* **1963**, *1*, 1147−1162.
(30) Niyogi, S.; Hamon, M. A.; Perea, D. E.; Kang, C. B.; Zhao, B.; Pal, S. K.; Wyant, A. E.; Itkis, M. E.; Haddon, R. C. *J. Phys. Chem. B* **2003**, *107*, 8799−8804.
(31) Du, F.; Fischer, J. E.; Winey, K. I. *Phys. Rev. B: Condens. Matter* **2005**, *72*, 121404/1−121404/4.
(32) Haggenmueller, R.; Fischer, J. E.; Winey, K. I. *Macromolecules* **2006**, *39*, 2964−2971.
(33) Aharoni, S. M. *n-Nylons: Their synthesis, structure and properties*; Wiley: New York, 1997.

NL062868E